

# 14 Linear Response and Electron-Phonon Coupling

Rolf Heid

Institute for Quantum Materials and Technologies  
Karlsruhe Institute of Technology

## Contents

<b>1</b>	<b>Introduction</b>	<b>2</b>
<b>2</b>	<b>Linear response in density functional theory</b>	<b>2</b>
2.1	Adiabatic perturbations . . . . .	2
2.2	Basics of density functional theory . . . . .	3
2.3	Linear-response formulation . . . . .	5
<b>3</b>	<b>Electron-phonon coupling</b>	<b>8</b>
3.1	General considerations . . . . .	8
3.2	Density functional perturbation theory . . . . .	9
<b>4</b>	<b>Applications</b>	<b>11</b>
4.1	Fröhlich Hamiltonian and many-body perturbation . . . . .	11
4.2	Renormalization of electronic properties . . . . .	13
4.3	Phonon renormalization . . . . .	16
4.4	Transport . . . . .	17
4.5	Phonon-mediated pairing . . . . .	19
<b>5</b>	<b>Extensions: LDA+U and beyond</b>	<b>22</b>
<b>6</b>	<b>Summary</b>	<b>26</b>

## 1 Introduction

Electron and phonon quasiparticles are the fundamental constituents of solids. Knowledge of their interaction provides deeper insight in many physical properties. In metals, the electron-phonon coupling (EPC) profoundly alters low-energy electronic excitations, and gives important contributions to transport and thermodynamic properties. Coupling to phonons creates naturally an attractive interaction among electronic quasiparticles, triggering eventually the occurrence of a superconducting state. Recent decades have seen the rise of powerful computational tools to calculate these fundamental properties from first principles. In particular, density functional theory (DFT) and its extensions have been very successful in providing a deeper understanding of materials properties.

The purpose of this lecture is to introduce the modern linear-response technique within the DFT framework, which gives access to EPC properties on a microscopic level, and to establish the connections to derived physical quantities. In Section 2, we will present an overview of the linear-response scheme, which is called density functional perturbation theory (DFPT). In Section 3, this approach is applied to the case of a crystalline solid, and we show how EPC properties can be calculated. Applications to various physical observables related to the EPC will be presented in Section 4. Finally, in Section 5, we will take a brief look at more complex extensions of DFT and how they can be used for an improved description of the EPC.

Throughout this Chapter, Rydberg atomic units  $\hbar=2m_e=e^2/2=1$  as well as  $k_B=1$  are used.

## 2 Linear response in density functional theory

In this Section, we will develop the machinery of the linear response in the context of density functional theory. The description will be kept rather general, but with having in mind to apply it to the case of a crystalline solid, which will be addressed in more detail in the following Section.

### 2.1 Adiabatic perturbations

There often exists an intimate relationship between physical observables and changes of ground state properties under perturbations. To be specific, let us consider interacting electrons moving in the potential of a periodic arrangement of atoms. In its ground state it has the energy  $E_0$ . This system can be perturbed in various ways. Examples are the displacement of an atom out of its equilibrium position  $\delta R$ , or a distortion of the crystal by applying a homogeneous strain  $\eta$ . Application of a homogeneous electric field,  $\mathbf{E}$  is a further example.

In all these cases, the perturbation can be arbitrarily small. The electronic system reacts adiabatically, if it remains in the ground state under a small perturbation  $\lambda$ . The ground state energy becomes a function of  $\lambda$ :  $E_0 = E_0(\lambda)$ . Many physical quantities are then linked directly to derivatives of this function,

$$Q_n = \left. \frac{d^n E}{d\lambda^n} \right|_{\lambda \rightarrow 0}. \quad (1)$$

type of perturbation $\lambda$	order $n$	physical property $Q$
displacements of atoms $\delta\mathbf{R}$	1	atomic force
	2	force constants
	$\geq 3$	anharmonic force constants
homogeneous strain $\eta$	1	stress
	2	elastic constants
	$\geq 3$	higher order elastic constants
homogeneous electric field $\mathbf{E}$	1	dipole moment
	2	polarizability
$\delta\mathbf{R} + \eta$	2+1	Grüneisen parameter
$\delta\mathbf{R} + \mathbf{E}$	1+2	Raman scattering cross section

**Table 1:** Examples of external perturbations and physical quantities connected to derivatives of the ground-state energy.

Table 1 lists examples of such relationships between perturbations and physical observables. Some physical quantities are connected to mixed derivatives of two different perturbations. A well known example is the Raman scattering cross section, which involves both atomic displacement and homogeneous electric field as perturbations.

Density functional theory is ideally suited to exploit this relationship between physical observables and derivatives of the ground-state energy, because it targets ground-state properties by design.

## 2.2 Basics of density functional theory

The foundations of density functional theory (DFT) have been laid in the seminal works by Hohenberg, Kohn, and Sham [1,2] in the mid 60's, and are outlined in numerous reviews [3–5]. Here we focus on the essential features which we need later.

Hohenberg and Kohn [1] proved, that the ground-state energy of a system of interacting electrons moving in an external potential  $v_{\text{ext}}(\mathbf{r})$  is obtained by minimizing the functional

$$E[n] = F[n] + \int d^3r v_{\text{ext}}(\mathbf{r}) n(\mathbf{r}) \quad (2)$$

with respect to the electron density  $n(\mathbf{r})$ . At its minimum,  $n(\mathbf{r})$  is the true electron density of the interacting system. The functional  $F[n]$  is universal, i.e., independent of the external potential. An important step for practical applications was done by Kohn and Sham [2]. By using the minimum principle they showed that one can define a fictitious system of non-interacting electrons, which in its ground state possesses the same inhomogeneous density as the interacting system [2]. The energy functional is expressed as

$$F[n] = T_s[n] + E_H[n] + E_{XC}[n], \quad (3)$$

where  $T_s$  represents the kinetic energy of the non-interacting electrons

$$T_s[n] = \sum_i f_i \int d^3r \psi_i^*(\mathbf{r}) (-\nabla^2) \psi_i(\mathbf{r}) \quad (4)$$

and  $E_H[n]$  the Hartree energy

$$E_H[n] = \int d^3r \int d^3r' \frac{n(\mathbf{r})n(\mathbf{r}')}{|\mathbf{r}-\mathbf{r}'|}. \quad (5)$$

The complexity of the original many-body problem is transferred to the exchange-correlation energy  $E_{XC}$ . It is also a functional of the density, and has the important property that it is universal and thus does not depend on the external potential. However, its functional form is in general unknown.

For the non-interacting electron system, the density can be expressed in terms of the single-particle wave functions  $\psi_i$ ,

$$n(\mathbf{r}) = \sum_i f_i |\psi_i(\mathbf{r})|^2, \quad (6)$$

where  $f_i$  denotes the occupation number of the state  $\psi_i$ .

From the variational property of the energy functional, one can derive the single-particle equation (Kohn-Sham equation)

$$\left(-\nabla^2 + v_{\text{eff}}(\mathbf{r})\right)\psi_i(\mathbf{r}) = \varepsilon_i \psi_i(\mathbf{r}). \quad (7)$$

Here,  $\varepsilon_i$  denotes the energy of the single-particle state  $\psi_i$ . The effective potential  $v_{\text{eff}}(\mathbf{r})$  is a functional of the density and given as a sum of the external potential and a screening potential

$$v_{\text{eff}}[n] = v_{\text{ext}} + v_{\text{scr}}[n] = v_{\text{ext}} + v_H[n] + v_{XC}[n]. \quad (8)$$

The latter is obtained as functional derivatives of the last two terms in the total energy functional (3). It consists of the Hartree potential

$$v_H(\mathbf{r})[n] = \frac{\delta E_H}{\delta n(\mathbf{r})} = \int d^3r' \frac{2n(\mathbf{r}')}{|\mathbf{r}-\mathbf{r}'|}, \quad (9)$$

which describes an average electrostatic potential originating from the other electrons, and the exchange-correlation potential  $v_{XC}(\mathbf{r}) = \delta E_{XC}/\delta n(\mathbf{r})$ .

Essentially, the original complex many-body problem is mapped onto a much simpler non-interacting electron system. The remaining task is to solve a set of single-particle equations (6)–(8), which has to be done in a self-consistent manner.

The big success of DFT partly rests on the empirical fact that already simple approximations to  $v_{XC}$  often give very accurate results. One ansatz is the local-density approximation (LDA)

$$v_{XC}^{LDA}(\mathbf{r}) = \left. \frac{d(n \varepsilon_{XC}^{\text{hom}}(n))}{dn} \right|_{n=n(\mathbf{r})}, \quad (10)$$

where  $\varepsilon_{XC}^{\text{hom}}(n)$  represents the exchange-correlation energy density of the homogeneous interacting electron gas. Another is the generalized-gradient approximation (GGA), where a dependence of  $v_{XC}$  on both local density and local gradient of the density is considered. For both types of local approximations, various parameterizations derived from analytical and numerical studies exist [4, 6–8].

## 2.3 Linear-response formulation

Here we show how the perturbative approach is set up within the DFT framework. We will first present some general considerations before applying them to the more specific cases in the next Section.

### 2.3.1 Energy derivatives

Let us consider a situation where the external potential  $v_{\text{ext}}$  depends on a set of adiabatic perturbation parameters  $\Lambda = \{\lambda_a, a = 1, \dots, p\}$ . Each  $v_{\text{ext}}^\Lambda$  determines an electronic ground state with density  $n^\Lambda(\mathbf{r})$ , for which the energy functional  $E^\Lambda[n] = F[n] + \int d^3r v_{\text{ext}}^\Lambda(\mathbf{r})n(\mathbf{r})$  is minimal

$$\left. \frac{\delta E^\Lambda[n]}{\delta n(\mathbf{r})} \right|_{n=n^\Lambda} = 0. \quad (11)$$

The ground-state energy is then given by

$$E_0^\Lambda = E^\Lambda[n^\Lambda] = F[n^\Lambda] + \int d^3r n^\Lambda(\mathbf{r})v_{\text{ext}}^\Lambda(\mathbf{r}), \quad (12)$$

which depends on the perturbation via the external potential and implicitly via the density. Its derivative then contains two contributions

$$\begin{aligned} \frac{\partial E_0^\Lambda}{\partial \lambda_a} &= \int d^3r n^\Lambda(\mathbf{r}) \frac{\partial v_{\text{ext}}^\Lambda(\mathbf{r})}{\partial \lambda_a} + \int d^3r \left. \frac{\delta E^\Lambda[n]}{\delta n(\mathbf{r})} \right|_{n=n^\Lambda} \frac{\partial n^\Lambda(\mathbf{r})}{\partial \lambda_a} \\ &= \int d^3r n^\Lambda(\mathbf{r}) \frac{\partial v_{\text{ext}}^\Lambda(\mathbf{r})}{\partial \lambda_a}. \end{aligned} \quad (13)$$

The second term vanishes because of Eq. (11). Thus the first derivative depends on the ground-state density only. This represents the DFT equivalent of the well known Hellmann-Feynman-Theorem [9].

Because Eq. (13) is valid for each finite  $\Lambda$ , one can take the second-order derivatives

$$\frac{\partial^2 E_0^\Lambda}{\partial \lambda_a \partial \lambda_b} = \int d^3r \frac{\partial n^\Lambda(\mathbf{r})}{\partial \lambda_b} \frac{\partial v_{\text{ext}}^\Lambda(\mathbf{r})}{\partial \lambda_a} + \int d^3r n^\Lambda(\mathbf{r}) \frac{\partial^2 v_{\text{ext}}^\Lambda(\mathbf{r})}{\partial \lambda_a \partial \lambda_b}. \quad (14)$$

Usually, the parametric dependence of  $v_{\text{ext}}^\Lambda$  on  $\Lambda$  is known, and its derivatives can be obtained easily. The hard part is to calculate the derivatives of the electron density. Eq. (14) demonstrates, that knowledge of the first-order variation of  $n$  is sufficient to access the second-order derivatives of the total energy. This aspect is very important for practical purposes, as one has to consider merely the linear response of the electron system.

As shown above, the first derivative of the energy depends solely of the unperturbed ground-state density, while second-order derivatives require knowledge of the density and its first-order derivatives. Both results are special cases of the so-called  $(2n+1)$  theorem, which states that all derivatives of the total energy up to  $(2n+1)$ -th order with respect to the adiabatic perturbation can be calculated from the knowledge of all derivatives of the Kohn-Sham eigenstates and density up to  $n$ -th order. The proof given by Gonze *et al.* [10–12] essentially rests on the variational property of the energy functional.

### 2.3.2 Linear response within the Kohn-Sham scheme

Let us now discuss how the linear response of the density is actually calculated with the DFT framework. It involves standard perturbation techniques under the condition that the effective potential entering the Kohn-Sham equations depends on the ground-state density. To this end we are interested in the linear response of the Kohn-Sham system

$$\left(-\nabla^2 + v_{\text{eff}}(\mathbf{r})\right)\psi_i(\mathbf{r}) = \varepsilon_i\psi_i(\mathbf{r}). \quad (15)$$

A small perturbation in the effective potential,  $\delta v_{\text{eff}}$ , gives rise to a first-order variation of the single-particle wave functions

$$\delta\psi_i(\mathbf{r}) = \sum_{j(\neq i)} \frac{\langle j|\delta v_{\text{eff}}|i\rangle}{\varepsilon_i - \varepsilon_j} \psi_j(\mathbf{r}). \quad (16)$$

Using a similar expression for  $\delta\psi_i^*(\mathbf{r})$  gives

$$\delta n(\mathbf{r}) = \sum_i f_i (\psi_i^*(\mathbf{r}) \delta\psi_i(\mathbf{r}) + \delta\psi_i^*(\mathbf{r}) \psi_i(\mathbf{r})) = \sum_{i\neq j} \frac{f_i - f_j}{\varepsilon_i - \varepsilon_j} \langle j|\delta v_{\text{eff}}|i\rangle \psi_i^*(\mathbf{r}) \psi_j(\mathbf{r}). \quad (17)$$

On the other hand,  $\delta n$  contributes to the variation of the effective potential

$$\begin{aligned} \delta v_{\text{eff}}(\mathbf{r}) &= \delta v_{\text{ext}}(\mathbf{r}) + \delta v_{\text{scr}}(\mathbf{r}) = \delta v_{\text{ext}}(\mathbf{r}) + \int d^3r' I(\mathbf{r}, \mathbf{r}') \delta n(\mathbf{r}') \\ I(\mathbf{r}, \mathbf{r}') &\equiv \frac{\delta v_{\text{scr}}(\mathbf{r})}{\delta n(\mathbf{r}')} = \frac{\delta v_{\text{H}}(\mathbf{r})}{\delta n(\mathbf{r}')} + \frac{\delta v_{\text{XC}}(\mathbf{r})}{\delta n(\mathbf{r}')} = \frac{2}{|\mathbf{r} - \mathbf{r}'|} + \frac{\delta^2 E_{\text{XC}}}{\delta n(\mathbf{r}) \delta n(\mathbf{r}')}. \end{aligned} \quad (18)$$

Eqs. (17) and (18) must be solved self-consistently to obtain the first-order variation of the density.

It is instructive to establish a relationship between  $\delta n$  and  $\delta v_{\text{ext}}$ . It can be derived by first writing the linear relationship (17) between  $\delta n$  and  $\delta v_{\text{eff}}$  more explicitly

$$\delta n(\mathbf{r}) = \int d^3r' \chi_0(\mathbf{r}, \mathbf{r}') \delta v_{\text{eff}}(\mathbf{r}') \quad (19)$$

$$\chi_0(\mathbf{r}, \mathbf{r}') = \sum_{i\neq j} \frac{f_i - f_j}{\varepsilon_i - \varepsilon_j} \psi_i^*(\mathbf{r}) \psi_j(\mathbf{r}) \psi_j^*(\mathbf{r}') \psi_i(\mathbf{r}'). \quad (20)$$

Here,  $\chi_0$  represents the charge susceptibility of the non-interacting Kohn-Sham system. It is expressed solely by ground-state quantities [13]. Although obtained by perturbation theory, Eq. (20) is exact because the Kohn-Sham equations describe non-interacting electrons.

In combination with Eq. (18) this leads to

$$\delta v_{\text{eff}} = \delta v_{\text{ext}} + I \chi_0 \delta v_{\text{eff}}, \quad (21)$$

which can be solved for  $\delta v_{\text{eff}}$

$$\delta v_{\text{eff}} = (1 - I \chi_0)^{-1} \delta v_{\text{ext}} = \epsilon^{-1} \delta v_{\text{ext}}, \quad (22)$$

where  $\epsilon = 1 - I \chi_0$  denotes the static dielectric matrix and describes the screening of the "bare" perturbation. Using Eq. (19), one finally arrives at

$$\delta n = \chi_0 \epsilon^{-1} \delta v_{\text{ext}}, \quad (23)$$

which in principle allows the calculation of the second derivative, Eq. (14).

The problem is now reduced to a calculation of  $\epsilon^{-1}$ . Direct evaluation of Eq. (23) has several caveats. Firstly, it involves inversion of the matrix  $\epsilon(\mathbf{r}, \mathbf{r}')$ , which for periodic systems is most conveniently done in Fourier space. It is, however, often numerically expensive, because a proper convergence requires a large number of Fourier components, and the size of the matrix becomes prohibitively large. Secondly, to obtain  $\chi_0$  via Eq. (20) involves summation also over unoccupied orbitals, which either converge slowly, or are not accessible at all, as in band-structure methods employing minimal basis sets (e.g. LMTO).

### 2.3.3 Modern formulation: Density functional perturbation theory

An important progress has been achieved by a new formulation of the linear-response approach, which avoids some of the aforementioned problems of the dielectric matrix approach. It is called density functional perturbation theory (DFPT) and has been proposed independently by Zein *et al.* [14–16] and Baroni *et al.* [17, 18]. A concise description can be found in [19]. We will give a short outline for the case of a non-metallic system.

In the expression (17) for the first-order density variation, the prefactor  $(f_i - f_j)/(\epsilon_i - \epsilon_j)$  restricts the sum to combinations where one state comes from the valence space and the other from the conduction space. Using time-reversal symmetry, this can be rewritten as

$$\delta n(\mathbf{r}) = 2 \sum_{vc} \frac{1}{\epsilon_v - \epsilon_c} \langle c | \delta v_{\text{eff}} | v \rangle \psi_v^*(\mathbf{r}) \psi_c(\mathbf{r}). \quad (24)$$

Now one defines the quantity

$$|\Delta_v\rangle = \sum_c \frac{1}{\epsilon_v - \epsilon_c} |c\rangle \langle c | \delta v_{\text{eff}} | v \rangle, \quad (25)$$

which collects the summation over the conduction bands. The linear response of the density is rewritten as

$$\delta n(\mathbf{r}) = 2 \sum_v \psi_v^*(\mathbf{r}) \Delta_v(\mathbf{r}). \quad (26)$$

To avoid an explicit evaluation of the sum in  $\Delta_v$ , one makes use of the following property

$$(H_{KS} - \epsilon_v) |\Delta_v\rangle = - \sum_c |c\rangle \langle c | \delta v_{\text{eff}} | v \rangle = -P_c \delta v_{\text{eff}} | v \rangle = (P_v - 1) \delta v_{\text{eff}} | v \rangle. \quad (27)$$

Here,  $H_{KS} = -\nabla^2 + v_{\text{eff}}$  is the KS Hamiltonian.  $P_c = \sum_c |c\rangle \langle c|$  denotes the projector onto the conduction space, and  $P_v = 1 - P_c$  the projector onto the valence space. Eq. (27) represents a linear equation for  $\Delta_v$ , where only valence-state quantities enter. Solution of this linear equation turns out to be numerically much more efficient than the expensive summation over conduction states.

In practice, Eqs. (26), (27) together with (18) define a set of self-consistent equations which is typically solved in an iterative manner.

### 3 Electron-phonon coupling

The most common application of DFT linear response approaches addresses the calculation of lattice dynamical properties, i.e., phonons, and their interaction with electrons. Here we discuss the underlying concepts.

#### 3.1 General considerations

Our starting point will be the adiabatic or Born-Oppenheimer approximation. The coupling between electrons and ions is governed by the large ratio of the ionic mass ( $M$ ) and electronic mass ( $m$ ). It allows a partial decoupling of the dynamics of the ions and the electrons by a systematic expansion in terms of the small parameter  $\kappa = (m/M)^{1/4}$  [20, 21]. To lowest order, the total wave function of the coupled electron-ion system can be written as a product  $\Psi(\underline{\mathbf{r}}, \underline{\mathbf{R}}) = \chi(\underline{\mathbf{R}})\psi(\underline{\mathbf{r}}; \underline{\mathbf{R}})$ , where  $\underline{\mathbf{r}}$  and  $\underline{\mathbf{R}}$  denote the sets of electron and ion coordinates, respectively. The electronic wave function obeys the equation

$$(T_e + V_{ee} + V_{e-i}(\underline{\mathbf{R}})) \psi_n(\underline{\mathbf{r}}; \underline{\mathbf{R}}) = E_n(\underline{\mathbf{R}}) \psi_n(\underline{\mathbf{r}}; \underline{\mathbf{R}}), \quad (28)$$

where  $T_e$  and  $V_{ee}$  denote the kinetic energy and Coulomb interaction of the electron system, respectively.  $V_{e-i}$  represents the electron-ion interaction. Through this term, wave functions and energies depend parametrically on the ionic positions  $\underline{\mathbf{R}}$ , and as a consequence also the electronic ground-state energy  $E_0(\underline{\mathbf{R}})$ . The latter enters the effective potential

$$\Omega(\underline{\mathbf{R}}) = V_{ii}(\underline{\mathbf{R}}) + E_0(\underline{\mathbf{R}}), \quad (29)$$

which governs the statics and dynamics of the ions in adiabatic approximation. Here  $V_{ii}(\underline{\mathbf{R}})$  denotes is the ion-ion (Coulomb) interaction.  $\Omega$  is the starting point of the microscopic theory of lattice dynamics (see review articles [22–24]). Dynamical properties are derived by a systematic expansion of  $\Omega$  in atom displacements  $\mathbf{u}$  around a chosen reference configuration,  $\mathbf{R}_i = \mathbf{R}_i^0 + \mathbf{u}_i$ , leading to

$$\Omega(\underline{\mathbf{R}}) = \Omega(\underline{\mathbf{R}}^0) + \sum_{i\alpha} \Phi_\alpha(i) u_{i\alpha} + \frac{1}{2} \sum_{i\alpha j\beta} \Phi_{\alpha\beta}(i, j) u_{i\alpha} u_{j\beta} + \dots \quad (30)$$

Greek indices  $\alpha$  and  $\beta$  denote Cartesian coordinates, while  $i$  and  $j$  are atom indices. The term of first order is the negative of the force acting on an atom in the reference configuration, i.e.,  $F_{i\alpha} = -\left. \frac{\partial \Omega}{\partial R_{i\alpha}} \right|_0 = -\Phi_\alpha(i)$ . It vanishes if one chooses as reference the equilibrium configuration, which minimizes  $\Omega$ . The second-order coefficients given by

$$\Phi_{\alpha\beta}(i, j) = \left. \frac{\partial^2 \Omega}{\partial R_{i\alpha} \partial R_{j\beta}} \right|_0 \quad (31)$$

are the so-called force constants.

To get a coupling of the dynamics of electrons and ions, one has to go beyond the adiabatic approximation. It is described by an electron-ion vertex and appears to first order in  $\kappa$ . One can

show that it results in off-diagonal matrix elements among the electronic eigenstates  $\psi_n$  and has the form

$$\langle n | \delta_{\mathbf{R}} V | n' \rangle. \quad (32)$$

The operator  $\delta_{\mathbf{R}} V$  stands for the linear change of the potential felt by the electrons under a displacement of an atom from its rest position.

In the following, we will show how these general considerations come to life within a density functional theory context. To this end, we will do this specifically for the very important case of a solid, i.e., a periodic arrangement of atoms.

## 3.2 Density functional perturbation theory

### 3.2.1 Phonon properties from DFPT

In adiabatic approximation, Eq. (28) describes interacting electrons moving in the potential determined by the ionic positions. This can be (approximately) solved by the DFT approach. We now consider the case of a solid, and assume that ions in their rest positions are sitting on a periodic lattice. KS eigenstates are now Bloch states  $|\mathbf{k}\nu\rangle$  characterized by momentum  $\mathbf{k}$  and band index  $\nu$ , respectively, and are solutions of  $H_{KS}|\mathbf{k}\nu\rangle = \varepsilon_{\mathbf{k}\nu}|\mathbf{k}\nu\rangle$ .

In a periodic crystal, ions are characterized by two indices  $i=(ls)$ , which denote the unit cell ( $l$ ) and the ions inside a unit cell ( $s$ ), respectively. For periodic boundary conditions, the Fourier transform of the force constant matrix is related to the dynamical matrix

$$D_{s\alpha s'\beta}(\mathbf{q}) = \frac{1}{\sqrt{M_s M_{s'}}} \sum_l \Phi_{\alpha\beta}(ls, 0s') e^{-i\mathbf{q}(\mathbf{R}_{ls}^0 - \mathbf{R}_{0s'}^0)}, \quad (33)$$

which determines the equation for the normal modes or phonons

$$\sum_{s'\beta} D_{s\alpha s'\beta}(\mathbf{q}) \eta_{s'\beta}(\mathbf{q}j) = \omega_{\mathbf{q}j}^2 \eta_{s\alpha}(\mathbf{q}j). \quad (34)$$

$\omega_{\mathbf{q}j}$  and  $\eta_{s\alpha}(\mathbf{q}j)$  denote the energy and polarization of the normal mode determined by the wavevector  $\mathbf{q}$  and the branch index  $j$ .

According to Eqs. (29) and (30), the force constants consist of two contributions, the ion-ion and the electronic contribution. The ion-ion part stems from the Coulomb interaction of ions positioned on a periodic lattice and can be evaluated with standard methods (Ewald summation). The second part comes from the second derivative of the electronic energy and is thus accessible by density functional perturbation theory. To this end we consider periodic displacements of the ions from their equilibrium positions,  $\mathbf{R}_{ls} = \mathbf{R}_{ls}^0 + \mathbf{u}_{ls}$ , of the form

$$u_{ls\alpha} = d_{s\alpha} e^{i\mathbf{q}\mathbf{R}_{ls}^0} + d_{s\alpha}^* e^{-i\mathbf{q}\mathbf{R}_{ls}^0}, \quad (35)$$

The complex amplitudes  $d_{s\alpha}$  allow to vary the relative phase of the displacement. It is convenient to denote the corresponding derivatives by  $\delta_{s\alpha}^{\mathbf{q}} \equiv \frac{\partial}{\partial d_{s\alpha}}$  and  $\delta_{s'\beta}^{-\mathbf{q}} \equiv \frac{\partial}{\partial d_{s'\beta}^*}$ . The electronic contribution to the dynamical matrix can be then written as a mixed derivative

$$D_{s\alpha s'\beta}(\mathbf{q}) = \frac{1}{\sqrt{M_s M_{s'}}} \delta_{s\alpha}^{\mathbf{q}} \delta_{s'\beta}^{-\mathbf{q}} E \Big|_{\mathbf{u}=0}. \quad (36)$$

Commonly, the external potential is expressed as a superposition of atomic potentials  $v_s$  centered at the instantaneous positions of the ions

$$v_{\text{ext}}(\mathbf{r}) = \sum_{l_s} v_s(\mathbf{r} - \mathbf{R}_{l_s}). \quad (37)$$

Its first-order variation, evaluated at the equilibrium positions, is given by

$$\delta_{s\alpha}^{\mathbf{q}} v_{\text{ext}}(\mathbf{r}) = - \sum_l \nabla_{\alpha}^{\mathbf{r}} v_s(\mathbf{r} - \mathbf{R}_{l_s}^0) e^{i\mathbf{q}\mathbf{R}_{l_s}^0} = -e^{i\mathbf{q}\mathbf{r}} \sum_l e^{i\mathbf{q}(\mathbf{R}_{l_s}^0 - \mathbf{r})} \nabla_{\alpha}^{\mathbf{r}} v_s(\mathbf{r} - \mathbf{R}_{l_s}^0). \quad (38)$$

The quantity defined by the lattice sum has the periodicity of the original lattice. Thus the derivative  $\delta_{s\alpha}^{\mathbf{q}}$  can be considered to carry a momentum  $\mathbf{q}$ .

When using a Bloch representation for the electronic eigenstates, the variation of the effective potential,  $\delta_{s\alpha}^{\mathbf{q}} v_{\text{eff}}$ , connects states of momentum  $\mathbf{k}$  with those of momentum  $\mathbf{k} + \mathbf{q}$ . The Fourier transform of the first order density variation takes the form

$$\delta_{s\alpha}^{\mathbf{q}} n(\mathbf{q} + \mathbf{G}) = -\frac{4}{V} \sum_{\mathbf{k}v} \langle \mathbf{k}v | e^{-i(\mathbf{q} + \mathbf{G})\mathbf{r}} | \Delta_{s\alpha}^{\mathbf{q}}(\mathbf{k}v) \rangle, \quad (39)$$

where  $V$  denotes the crystal volume. The quantity appearing on the right hand side is closely related to the first-order variation of the valence state  $|\mathbf{k}v\rangle$  and is defined by (see Eq. (25))

$$|\Delta_{s\alpha}^{\mathbf{q}}(\mathbf{k}v)\rangle = \sum_c \frac{|\mathbf{k} + \mathbf{q}c\rangle \langle \mathbf{k} + \mathbf{q}c | \delta_{s\alpha}^{\mathbf{q}} v_{\text{eff}} | \mathbf{k}v \rangle}{\varepsilon_{\mathbf{k} + \mathbf{q}c} - \varepsilon_{\mathbf{k}v}}. \quad (40)$$

It is obtained by solving the inhomogeneous linear equations (see Eq. (27))

$$(H_{KS} - \varepsilon_{\mathbf{k}v}) |\Delta_{s\alpha}^{\mathbf{q}}(\mathbf{k}v)\rangle = (P_v^{\mathbf{k} + \mathbf{q}} - 1) \delta_{s\alpha}^{\mathbf{q}} v_{\text{eff}} | \mathbf{k}v \rangle. \quad (41)$$

Eqs. (39) and (41) together with (18) constitute a set of equations, which is solved self-consistently for a fixed  $\mathbf{q}$  to obtain  $\delta_{s\alpha}^{\mathbf{q}} n$ . As a by-product, also  $\delta_{s\alpha}^{\mathbf{q}} v_{\text{eff}}$  is calculated.

The electronic contribution to the dynamical matrix takes the form

$$\delta_{s\alpha}^{\mathbf{q}} \delta_{s'\beta}^{-\mathbf{q}} E = \sum_{\mathbf{G}} [\delta_{s\alpha}^{\mathbf{q}} n(\mathbf{G} + \mathbf{q}) \delta_{s'\beta}^{-\mathbf{q}} v_{\text{ext}}(\mathbf{G} + \mathbf{q}) + \delta_{s\alpha}^{\mathbf{q}} \delta_{s'\beta}^{-\mathbf{q}} v_{\text{ext}}(\mathbf{G})]. \quad (42)$$

### 3.2.2 Electron-phonon vertex from DFPT

We have seen that the lowest-order electron-ion interaction describes scattering of electronic states via the operator  $\delta_{\mathbf{R}} V$  which denotes the change of the potential felt by the electrons due to an ionic displacement. If the potential  $V$  is the bare electron-ion potential  $V^0$ , then  $\delta_{\mathbf{R}} V = \nabla V^0|_{\mathbf{R}_0} \mathbf{u}$ . In the context of DFPT, Eq. (32) would then be identified with

$$g_{\mathbf{k} + \mathbf{q}\nu', \mathbf{k}\nu}^{\mathbf{q}\lambda} = \sum_{s\alpha} A_{s\alpha}^{\mathbf{q}j} \langle \mathbf{k} + \mathbf{q}\nu' | \delta_{s\alpha}^{\mathbf{q}} v_{\text{ext}} | \mathbf{k}\nu \rangle \quad \text{with} \quad A_{s\alpha}^{\mathbf{q}j} = \frac{\eta_{s\alpha}(\mathbf{q}j)}{\sqrt{2M_s\omega_{\mathbf{q}j}}}, \quad (43)$$

where a transformation to the normal-mode coordinates is performed. Physically,  $g$  represents the probability amplitude of scattering a single electron by a simultaneous creation or annihilation of a single phonon. In the form given above this is called the bare vertex.

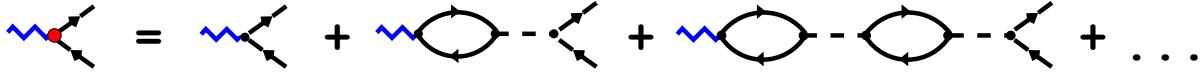


**Fig. 1:** Diagrammatic representation of the screened electron-phonon vertex within the DFPT framework. Blue zigzag lines represent phonons, black lines electron propagators, and the dashed lines the effective electron-electron interaction.

However, in solids, and in particular in metals, the bare electron-ion potential is screened by the other electrons. Screening also alters the vertex significantly. Within linear response theory this operator takes the form

$$\delta_{\mathbf{R}}V = \epsilon^{-1} \nabla V^0|_{\mathbf{R}_0} \mathbf{u}. \quad (44)$$

$\epsilon^{-1}$  is the inverse dielectric matrix, which is a measure of the screening. Note that in Eq. (44), the screening operator does not commute with the gradient operation, and thus can not be written in terms of the gradient of a screened potential.

It is instructive to look at it from a many-body perturbation perspective. Fig. 1 shows a diagrammatic representation of the screened vertex. The bare vertex is given by the first graph on the right hand side, and is screened by virtual electron-hole excitations coupled via an effective interaction. From the relationship (21) between the external (bare) and effective (screened) perturbation, we can see that within the DFPT framework, the electron-hole bubble is represented by the charge-susceptibility of the non-interaction Kohn-Sham system (20). The effective interaction is given by the kernel  $I$  defined in Eq. (18) and incorporates besides the Coulomb interaction also contributions from exchange and correlation.

In essence this leads to a replacement of the external potential by the screened or effective one

$$g_{\mathbf{k}+\mathbf{q}\nu',\mathbf{k}\nu}^{\mathbf{q}\lambda} = \sum_{s\alpha} A_{s\alpha}^{\mathbf{q}j} \langle \mathbf{k}+\mathbf{q}\nu' | \delta_{s\alpha}^{\mathbf{q}} v_{\text{eff}} | \mathbf{k}\nu \rangle. \quad (45)$$

Applying the self-consistent procedure described above results in the linear response of the effective potential  $\delta_{s\alpha}^{\mathbf{q}} v_{\text{eff}}$ , which is then used to calculate the electron-phonon matrix elements. The self-consistency procedure automatically takes into account the important screening effects. Eq. (45) thus enables the calculation of the screened EPC matrix elements on a microscopic level, including their full momentum dependence and resolving the contributions from different electronic bands and phononic modes. For further details one can refer to the book of Grimvall [25].

## 4 Applications

### 4.1 Fröhlich Hamiltonian and many-body perturbation

When developing a perturbative treatment of the mutual influence of the electronic and phononic subsystems in a solid, the question arises, what are the proper noninteracting quasiparticles to start with. The correct answer requires to know the solution to some extent. As we will see, electronic states are significantly influenced by lattice vibrations mostly in close vicinity of the

Fermi energy. It is therefore appropriate to start with electrons moving in a static potential of a rigid ion lattice, without any renormalization by the lattice vibrations. On contrast, the bare vibrations of the ion lattice would be a bad starting point, because they are strongly altered by the screening of the electrons. This screening must be built into the description of the harmonic lattice vibrations which defines the noninteracting phonons.

Therefore, a good starting point is the *Fröhlich Hamiltonian*, which in second quantization reads

$$H = H_e + H_{ph} + H_{e-ph}. \quad (46)$$

The electron system is described by noninteracting quasi-particles with dispersion  $\varepsilon_{\mathbf{k}\nu}$ . These quasiparticles are considered to be the stationary solutions of band electrons in a perfect periodic lattice, and include already renormalization from Coulomb interaction.

$$H_e = \sum_{\mathbf{k}\nu\sigma} \varepsilon_{\mathbf{k}\nu} c_{\mathbf{k}\nu\sigma}^\dagger c_{\mathbf{k}\nu\sigma}. \quad (47)$$

Here  $c_{\mathbf{k}\nu\sigma}$  ( $c_{\mathbf{k}\nu\sigma}^\dagger$ ) are the annihilation (creation) operators for an electronic state with momentum  $\mathbf{k}$ , band index  $\nu$ , spin  $\sigma$ , and band energy  $\varepsilon_{\mathbf{k}\nu}$ .

The lattice Hamiltonian is expressed in terms of quantized harmonic vibrations, and represents noninteracting phonons

$$H_{ph} = \sum_{\mathbf{q}j} \omega_{\mathbf{q}j} \left( b_{\mathbf{q}j}^\dagger b_{\mathbf{q}j} + \frac{1}{2} \right), \quad (48)$$

where  $b_{\mathbf{q}j}$  ( $b_{\mathbf{q}j}^\dagger$ ) are the annihilation (creation) operators for a phonon with momentum  $\mathbf{q}$ , branch index  $j$ , and energy  $\omega_{\mathbf{q}j}$ . Phonons are the quanta of the normal mode vibrations. The operator of atom displacements is expressed as  $u_{l s \alpha} = e^{i\mathbf{q}\mathbf{R}_{ls}^0} / \sqrt{N_q} \sum_{\mathbf{q}j} A_{s\alpha}^{\mathbf{q}j} (b_{\mathbf{q}j} + b_{-\mathbf{q}j}^\dagger)$ , where  $N_q$  is the number of points in the summation over  $\mathbf{q}$ .

The third term describes the lowest-order coupling between electrons and phonons,

$$H_{e-ph} = \sum_{\mathbf{k}\nu\nu'\sigma} \sum_{\mathbf{q}j} g_{\mathbf{k}+\mathbf{q}\nu',\mathbf{k}\nu}^{\mathbf{q}j} c_{\mathbf{k}+\mathbf{q}\nu'\sigma}^\dagger c_{\mathbf{k}\nu\sigma} \left( b_{\mathbf{q}j} + b_{-\mathbf{q}j}^\dagger \right). \quad (49)$$

$g_{\mathbf{k}+\mathbf{q}\nu',\mathbf{k}\nu}^{\mathbf{q}j}$  is the electron-phonon matrix element, Eq. (45) and describes the probability amplitude for scattering an electron with momentum  $\mathbf{k}$  from band  $\nu$  to a state with momentum  $\mathbf{k}+\mathbf{q}$  in band  $\nu'$  under the simultaneous absorption (emission) of a phonon with momentum  $\mathbf{q}$  ( $-\mathbf{q}$ ) and branch index  $j$ .

To simplify the treatment, we will use a compact notation combining momentum and band or branch index into a single symbol:  $k=(\mathbf{k}\nu)$ ,  $k'=(\mathbf{k}'\nu')$ , and  $q=(\mathbf{q}j)$ . The EPC matrix elements are then denoted as

$$g_{k',k}^q = g_{\mathbf{k}'\nu',\mathbf{k}\nu}^{\mathbf{q}j} \delta_{\mathbf{k}',\mathbf{k}+\mathbf{q}}, \quad (50)$$

which implicitly takes into account momentum conservation.

This general form of the Fröhlich Hamiltonian is the starting point for a many-body perturbation theory [26], where  $H_0 = H_e + H_{ph}$  denotes the Hamiltonian of the unperturbed quasiparticles, and  $H_{e-ph}$  represents the perturbational part.

The bare Green functions of the unperturbed Hamiltonian  $H_0 = H_e + H_{ph}$  are

$$G_0(k, i\omega_n) = \frac{1}{i\omega_n - \varepsilon_k} \quad (51)$$

$$D_0(q, i\nu_m) = \frac{1}{i\nu_m - \omega_q} - \frac{1}{i\nu_m + \omega_q}. \quad (52)$$

where  $\omega_n = (2n+1)\pi T$  and  $\nu_m = 2m\pi T$ , with  $n, m$  integer values, denote fermionic and bosonic Matsubara frequencies, respectively. Electronic energies are measured with respect to the chemical potential. The Dyson equations

$$G(k, i\omega_n)^{-1} = G_0(k, i\omega_n)^{-1} - \Sigma(k, i\omega_n) \quad (53)$$

$$D(q, i\nu_m)^{-1} = G_0(q, i\nu_m)^{-1} - \Pi(q, i\nu_m) \quad (54)$$

connect bare and renormalized Green functions via the electron and phonon self-energy,  $\Sigma$  and  $\Pi$ , respectively. In the following we will have a closer look at the leading contributions of EPC to these electron and phonon self-energies.

## 4.2 Renormalization of electronic properties

The lowest-order diagram of the electron self-energy represents a virtual exchange of a phonon

$$\Sigma_{ep}(k, i\omega_n) = -T \sum_m \frac{1}{N_q} \sum_{k', q} g_{k', k}^q G_0(k', i\omega_n - i\nu_m) (g_{k', k}^q)^* D_0(q, i\nu_m). \quad (55)$$

After performing the Matsubara sum over  $\nu_m$  one obtains

$$\Sigma_{ep}(k, i\omega_n) = \frac{1}{N_q} \sum_{k', q} |g_{k', k}^q|^2 \left( \frac{b(\omega_q) + f(\varepsilon_{k'})}{i\omega_n + \omega_q - \varepsilon_{k'}} + \frac{b(\omega_q) + 1 - f(\varepsilon_{k'})}{i\omega_n - \omega_q - \varepsilon_{k'}} \right). \quad (56)$$

$\Sigma_{ep}$  depends on temperature  $T$  via the Fermi and Bose distribution functions,  $f(\varepsilon) = (e^{\varepsilon/T} + 1)^{-1}$  and  $b(\omega) = (e^{\omega/T} - 1)^{-1}$ , respectively.

To discuss the quasiparticle renormalization, we consider the retarded Green function, which is obtained by analytic continuation of Eq. (53) to real axis via  $i\omega_n \rightarrow \varepsilon + i\delta$  with an infinitesimal positive  $\delta$ . It is connected to the analytic continuation of the self-energy via the Dyson equation

$$G(k, \varepsilon) = (\varepsilon - \varepsilon_k - \Sigma(k, \varepsilon))^{-1}. \quad (57)$$

It is straightforward to perform the analytic continuation of  $\Sigma_{ep}(k, i\omega_n \rightarrow \varepsilon + i\delta)$  in the form given in Eq. (56) and to derive the expression for the imaginary part

$$\text{Im}\Sigma_{ep}(k, \varepsilon) = -\frac{\pi}{N_q} \sum_{k', q} |g_{k', k}^q|^2 \left( \delta(\varepsilon - \varepsilon_{k'} + \omega_q) (b(\omega_q) + f(\varepsilon_{k'})) + \delta(\varepsilon - \varepsilon_{k'} - \omega_q) (b(\omega_q) + 1 - f(\varepsilon_{k'})) \right) \quad (58)$$

It determines the quasiparticle linewidth (inverse lifetime) by

$$\Gamma_k = -2\text{Im}\Sigma(k, \bar{\varepsilon}_k), \quad (59)$$

while the shifted quasiparticle energy is determined by the real part via  $\bar{\varepsilon}_k = \varepsilon_k - \text{Re}\Sigma(k, \bar{\varepsilon}_k)$ .  $\text{Re}\Sigma_{ep}$  is obtained via the Kramers-Kronig relation  $\text{Re}\Sigma_{ep}(k, \varepsilon) = 1/\pi \int d\varepsilon' \text{Im}\Sigma_{ep}(k, \varepsilon')/(\varepsilon - \varepsilon')$ . This can be rewritten by introducing two spectral functions

$$\alpha^2 F_k^\pm(\varepsilon, \omega) = \frac{1}{N_q} \sum_q \delta(\omega - \omega_q) \sum_{k'} |g_{k',k}^q|^2 \delta(\varepsilon - \varepsilon_{k'} \pm \omega). \quad (60)$$

They depend on the electronic state  $k$  via the EPC vertex. The imaginary part can then be cast in the form

$$\text{Im}\Sigma_{ep}(k, \varepsilon) = -\pi \int_0^\infty d\omega \left( \alpha^2 F_k^+(\varepsilon, \omega) (b(\omega) + f(\omega + \varepsilon)) + \alpha^2 F_k^-(\varepsilon, \omega) (b(\omega) + f(\omega - \varepsilon)) \right). \quad (61)$$

The physical interpretation of this expression is as follows. When a quasiparticle hole is created at the state  $k$  ( $\varepsilon < \varepsilon_F$ ), electrons can scatter from states with higher or lower energies, respectively, accompanied by either emission or absorption of a phonon. The probabilities are given by  $\alpha^2 F_k^-$  and  $\alpha^2 F_k^+$ , respectively, weighted with the appropriate bosonic and fermionic distribution functions. A similar description holds when a quasiparticle (electron) is created at energies above the Fermi level.

Due to the small scale of the phonon energies, emission and absorption spectra are often rather similar as one can ignore the phonon energy  $\omega_q$  in the  $\delta$ -function of (60). Then

$$\alpha^2 F_k^\pm \approx \alpha^2 F_k(\varepsilon, \omega) = \frac{1}{N_q} \sum_q \delta(\omega - \omega_q) \sum_{k'} |g_{k',k}^q|^2 \delta(\varepsilon - \varepsilon_{k'}). \quad (62)$$

For this *quasielastic approximation* the expression for the EPC-induced linewidth simplifies to

$$\Gamma_k = \pi \int_0^\infty d\omega \left( \alpha^2 F_k(\bar{\varepsilon}_k, \omega) (2b(\omega) + f(\omega + \bar{\varepsilon}_k) + f(\omega - \bar{\varepsilon}_k)) \right). \quad (63)$$

The spectral function  $\alpha^2 F_k$  contains the essential information related to the electron-phonon coupling of the specific electronic state  $k = (\mathbf{k}\nu)$ . A convenient measure for the strength of the EPC is the dimensionless coupling parameter

$$\lambda_k = 2 \int d\omega \frac{\alpha^2 F_k(\varepsilon_k, \omega)}{\omega}. \quad (64)$$

It characterizes the strength of the coupling of a specific electronic state to the whole phonon spectrum, and depends both on the momentum and band character of the electronic state.

An example for a calculation of  $\lambda_k$  is given in Fig. 2. The topological insulator  $\text{Bi}_2\text{Se}_3$  possesses at its (0001) surface a metallic surface state with a very characteristic dispersion, a so-called Dirac cone. Its origin lies in the topological nature of the bulk band structure, and has very unusual properties, in particular a peculiar spin polarization. The study showed that the EPC coupling constant increases linearly with energy for states in the upper cone, but remains

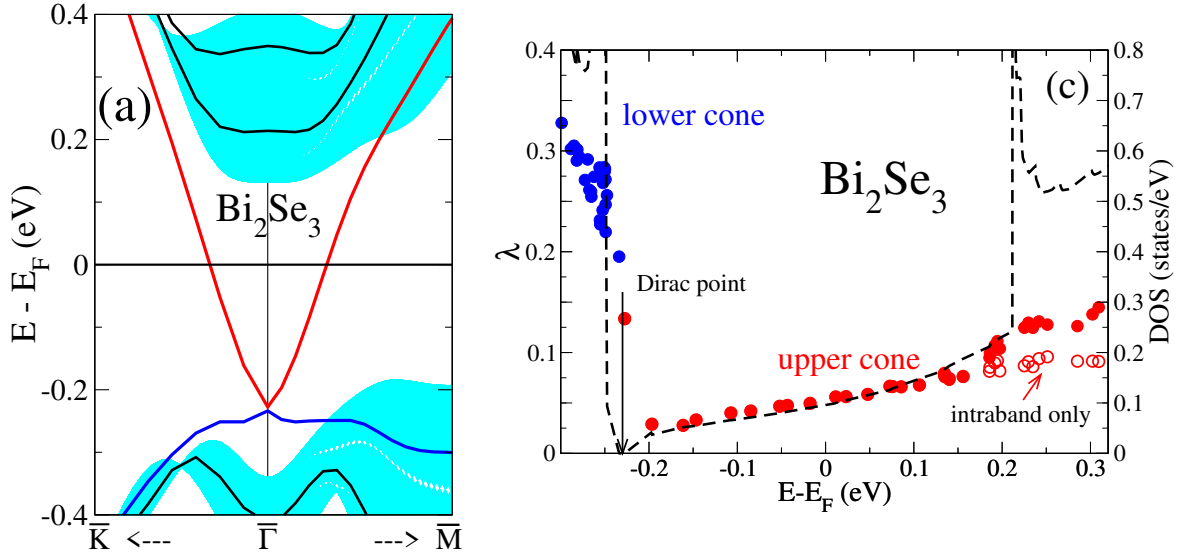


**Fig. 2:** Renormalization of electronic states in the surface Dirac cone of the topological insulator  $\text{Bi}_2\text{Se}_3$ . Calculations were done for a slab consisting of 3 quintuple layers (QL) separated by a large vacuum. (a) Bandstructure of the (0001) surface; shaded area indicated surface-projected bulk states. (b) Coupling constants of electronic states as function of binding energy. After [27].

small enough ( $\lambda < 0.15$ ), such that the electronic quasiparticles are not much disturbed by the coupling to phonons [27].

There are two relations which connect this parameter to experimentally accessible quantities. The first is related to the real part of the self-energy for an electronic band crossing the Fermi level

$$\lambda_k = \left. \frac{\partial \text{Re} \Sigma_{ep}(k, \varepsilon)}{\partial \varepsilon} \right|_{\varepsilon=0_F, T=0}. \quad (65)$$

Thus the coupling constant is given by the slope of  $\text{Re} \Sigma_{ep}$  right at the Fermi energy in the limit  $T \rightarrow 0$ .  $\lambda_k$  is also called the mass-enhancement parameter, because the quasiparticle velocity is changed to  $v_k^* = v_k / (1 + \lambda_k)$  and can be interpreted as an enhanced effective mass  $m_k^* = m_k (1 + \lambda_k)$ , where  $m_k$  denotes the unrenormalized mass. Eq. (65) is often utilized in ARPES measurements of bands crossing the Fermi level, which attempt to extract the energy dependence of the real part of the self-energy.

A second route to determine the coupling constant of an electronic state is via the temperature dependence of the linewidth. In Eq. (63), the  $T$ -dependence it contained solely in the Bose and Fermi distribution functions. For temperatures larger than the maximum phonon frequencies, it becomes almost linear in  $T$ , and its slope is determined by the average coupling parameter defined above

$$\Gamma_k \approx 2\pi \lambda_k T. \quad (66)$$

This relationship has been widely used to extract  $\lambda_k$  from measurements of  $\Gamma_k(T)$ , in particular for surface electronic states.

### 4.3 Phonon renormalization

The EPC also renormalizes the phononic quasiparticles. Measurement of the phonon linewidth provides another way to gain experimental information about the coupling strength. We will briefly sketch this approach here.

The finite linewidth  $\gamma_q$  (half-width at half maximum), or inverse lifetime of a phonon mode is connected to the imaginary part of the phonon self-energy by  $\gamma_q = -2\text{Im}\Pi_q(\omega_q)$ . The leading contributing to  $\Pi_q(\omega)$  is given by virtual electron-hole excitations expressed as

$$\begin{aligned}\Pi_q(i\nu_m) &= T \sum_n \frac{1}{N_k} \sum_{k,k'} |g_{k',k}^q|^2 G_0(k, i\omega_n) G_0(k'\nu', i\omega_n + i\nu_m) \\ &= \frac{1}{N_k} \sum_{k',k} |g_{k',k}^q|^2 \frac{f(\varepsilon_k) - f(\varepsilon_{k'})}{i\nu_m + \varepsilon_k - \varepsilon_{k'}}.\end{aligned}\quad (67)$$

Analytic continuation results in

$$\gamma_q = 2\pi \frac{1}{N_k} \sum_{k',k} |g_{k',k}^q|^2 (f(\varepsilon_k) - f(\varepsilon_{k'})) \delta(\omega_q + (\varepsilon_k - \varepsilon_{k'})). \quad (68)$$

This expression contains the  $T$ -dependence via the Fermi distribution functions  $f$ . Because phonon energies are typically small compared to electronic energies, the energy difference  $\varepsilon_k - \varepsilon_{k'}$  is also small, and one can approximate

$$f(\varepsilon_k) - f(\varepsilon_{k'}) \approx f'(\varepsilon_k) (\varepsilon_k - \varepsilon_{k'}) \rightarrow -f'(\varepsilon_k) \omega_q \quad (69)$$

with  $f' = df/d\varepsilon$ . In the limit  $T \rightarrow 0$ ,  $f'(\varepsilon_k) \rightarrow -\delta(\varepsilon_k)$ , and by neglecting  $\omega_q$  inside the  $\delta$ -function, the expression further simplifies to

$$\gamma_q = 2\pi \omega_q \frac{1}{N_k} \sum_{k',k} |g_{k',k}^q|^2 \delta(\varepsilon_k) \delta(\varepsilon_{k'}). \quad (70)$$

This approximate formula for the linewidth, first derived by Allen [28], is widely used in numerical calculations. As will be discussed below,  $\gamma_q$  in the form of Eq. (70) enters directly the expression for the coupling strength of a phonon mode relevant for superconductivity. Thus measurements of the phonon linewidths, for example by inelastic neutron or x-ray scattering experiments, provide information about the importance of a phonon mode for the pairing. One has to keep in mind, however, that  $\gamma_q$  only represents the contribution from EPC, while the experimental linewidth also contains other contributions like those from anharmonic decay processes. Furthermore, approximation (70) does not hold in the limit  $q \rightarrow 0$  for metals, because the phonon frequency in Eq. (68) cannot be neglected anymore for intraband contributions, which involve arbitrarily small energy differences  $\varepsilon_k - \varepsilon_{k'}$ .

An example of a combined study of EPC by DFPT and neutron-scattering experiments is shown in Fig. 3 for  $\text{YNi}_2\text{B}_2\text{C}$  [29, 30]. This member of the nickelborocarbide family is a strong coupling superconductor ( $T_C=15.2$  K), and exhibits pronounced phonon anomalies related to large and momentum dependent EPC. Good agreement for both renormalized phonon frequencies and linewidths as function of momentum indicates a good predictive power of the DFPT calculation for this compound.

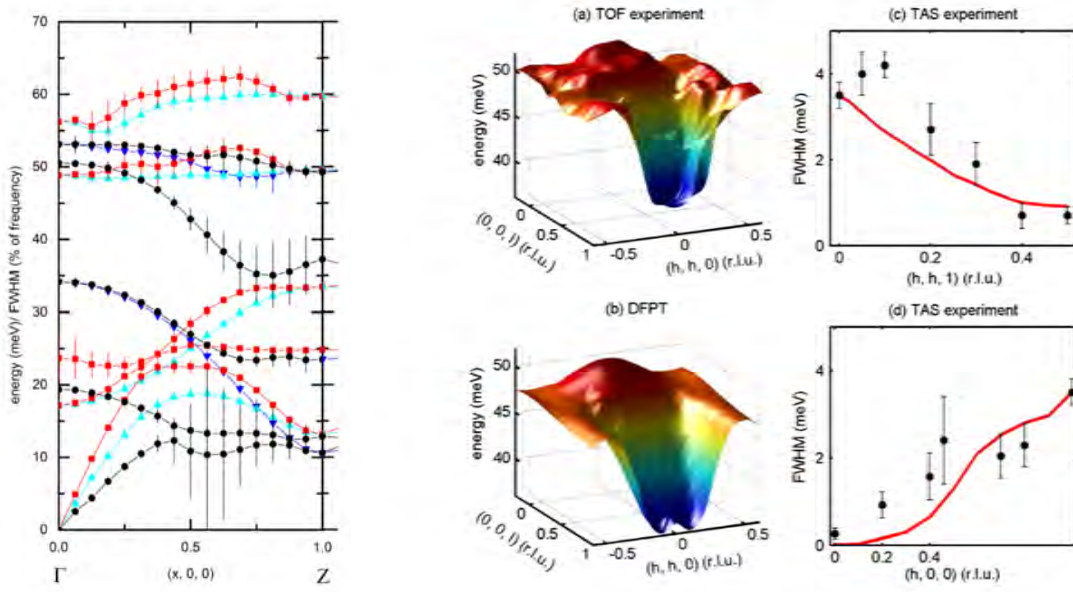


**Fig. 3:** Lattice dynamics of  $YNi_2B_2C$ . Left panel: theoretical phonon dispersion and linewidths (vertical bars) from DFPT. Right panel: time-of-flight neutron scattering results for the dispersion (a) and linewidth (c) of a prominent phonon branch compared with predictions from DFPT in (b) and (d), respectively. After [29, 30].

#### 4.4 Transport

The electron-phonon interaction plays an important role for electronic transport properties. The general approach is based on Boltzmann transport theory (see, e.g., [25, 31–33]) and is briefly sketched in the following. To be specific, we discuss the contribution of the EPC to the case of electrical conductivity. In a semi-classical picture, when one applies an external electric field  $\mathbf{E}$ , electrons become accelerated. By collisions with other objects (like defects, phonons or other electrons) they are scattered, until finally a steady state is reached. It is characterized by a new distribution  $F_k$  which differs from the Fermi distribution  $f_k = f(\varepsilon_k)$  in equilibrium. Knowledge of  $F_k$  allows to calculate the electronic current density via (for definiteness, we assume a field along  $x$ )

$$j_x = -\frac{2e}{V} \frac{1}{N_k} \sum_k F_k (v_k)_x \quad (71)$$

and the diagonal component of the electrical conductivity  $\sigma_{xx} = j_x/E_x$

The new occupation  $F_k$  is determined using the well known Boltzmann transport equation

$$-eE \frac{\partial F_k}{\partial k_x} = \left( \frac{\partial F_k}{\partial t} \right)_{\text{coll}}. \quad (72)$$

The left-hand side describes the change in occupations induced by the electric field, which is balanced by the rate of change of the occupation due to collisions given on the right-hand side.

Using Fermi golden rule the latter is expressed as

$$\left( \frac{\partial F_k}{\partial t} \right)_{\text{coll}} = \sum_{k'} \left( P_{k'k} F_{k'} (1-F_k) - P_{kk'} F_k (1-F_{k'}) \right). \quad (73)$$

Here,  $P_{kk'}$  denotes the probability of scattering an electron from state ( $k$ ) to ( $k'$ ). The first term ( $\propto P_{k'k}$ ) describes events, where electrons are scattered into state ( $k$ ), and the second those, where electrons are scattered out of that state.  $P_{kk'}$  must satisfy a detailed balance condition

$$P_{k'k} f_{k'} (1-f_k) = P_{kk'} f_k (1-f_{k'}) \quad (74)$$

such that the RHS of Eq. (72) vanishes in equilibrium.

When the scattering process is due to the electron-phonon interaction, the probability depends on the EPC vertex and the availability of phonons

$$P_{kk'} = \frac{2\pi}{N} |g_{k'k}^q|^2 \left( b(\omega_q) \delta(\varepsilon_{k'} - \varepsilon_k - \omega_q) + (b(\omega_q) + 1) \delta(\varepsilon_{k'} - \varepsilon_k + \omega_q) \right) \quad (75)$$

The first term describes a phonon annihilation, the second a phonon creation process.

For small applied fields, it is sufficient to look at the first-order change of the occupation with the electric field  $E_x$

$$F_k = f_k + f_k^1, \quad f_k^1 \propto E_x \quad (76)$$

and to resort to the linearized Boltzmann equation, where the left-hand side is approximated by

$$-eE_x \frac{\partial F_k}{\partial k_x} \rightarrow -eE_x \frac{\partial f_k}{\partial k_x} = -eE_x \frac{\partial f_k}{\partial \varepsilon_k} \frac{\partial \varepsilon_k}{\partial k_x} = -eE_x \frac{\partial f_k}{\partial \varepsilon_k} (v_k)_x. \quad (77)$$

The right-hand side simplifies in  $\mathcal{O}(E_x)$  to

$$\begin{aligned} & \sum_{k'} \left( P_{k'k} (f_{k'}^1 (1-f_k) - f_{k'} f_k^1) - P_{kk'} (f_k^1 (1-f_{k'}) - f_k f_{k'}^1) \right) \\ &= \sum_{k'} \left( -f_k^1 (P_{k'k} f_{k'} + P_{kk'} (1-f_{k'})) + f_{k'}^1 (P_{k'k} (1-f_k) + P_{kk'} f_k) \right) \\ &= \sum_{k'} P_{kk'} \left( -f_k^1 \frac{1-f_{k'}}{1-f_k} + f_{k'}^1 \frac{f_k}{f_{k'}} \right) \end{aligned} \quad (78)$$

In the last step, use of the detailed balance relation (74) was made.

To proceed further, one applies the so-called *energy relaxation time approximation*. It consists of neglecting the occupation changes of the in-scattered electrons:  $f_{k'}^1 = 0$ . Then the RHS consists only of the first term, which using Eq. (75) just gives  $-f_k^1/\tau_k$ . Here  $\tau_k = 1/\Gamma_k$  is the lifetime or inverse linewidth of the electronic state ( $k$ ) as derived in Eq. (63). Now the linearized Boltzmann equations with (76) and (77) can be solved easily

$$f_k^1 = eE_x \frac{\partial f_k}{\partial \varepsilon_k} (v_k)_x \tau_k \quad (79)$$

which finally gives for the conductivity

$$\sigma_{xx} = -\frac{2e}{VE_x} \frac{1}{N_k} \sum_k F_k (v_k)_x = -\frac{2e}{VE_x} \frac{1}{N_k} \sum_k f_k^1 (v_k)_x = \frac{2e^2}{V} \frac{1}{N_k} \sum_k \left( -\frac{\partial f_k}{\partial \varepsilon_k} \right) (v_k)_x (v_k)_x \tau_k \quad (80)$$

Direct evaluation of this equation from first principles is quite demanding, as it requires the calculation of  $V_k$  and in particular  $\tau_k$  for each relevant  $k$ . It has been used to assess the mobility of carriers in doped semiconductors [34, 35].

For metals, a simplified expression often works very well. Here, the  $k$ -dependent lifetime is replaced by an effective relaxation time  $\tau$ , which is determined using a variational procedure to solve the Boltzmann equation [31]. In the case of pure electron-phonon scattering, it takes the form [36–38]

$$\frac{1}{\tau} = 2\pi \int dx \frac{x}{\sinh^2 x} \alpha_{\text{tr}}^2 F(\omega) \quad (81)$$

with  $x = \omega/2T$ . The properties of the electron-phonon scattering are encoded in the transport spectral function

$$\alpha_{\text{tr}}^2 F(\omega) = \frac{1}{N_q} \sum_q \delta(\omega - \omega_q) \frac{1}{N(0)} \frac{1}{N_k} \sum_{kk'} |g_{k'k}^q|^2 \eta_{k'k} \delta(\varepsilon_k) \delta(\varepsilon_{k'}), \quad (82)$$

where  $N(0) = 1/N_k \sum_k \delta(\varepsilon_k)$  is the electronic density of states per spin at the Fermi energy.  $\alpha_{\text{tr}}^2 F(\omega)$  is very similar to the isotropic Eliashberg function  $\alpha^2 F$  appearing in the theory of phonon-mediated superconductivity (see Eq. (87)). The only difference lies in the efficiency factor

$$\eta_{k'k} = 1 - \frac{\mathbf{v}_k \mathbf{v}_{k'}}{|\mathbf{v}_k|^2}, \quad (83)$$

which accounts for a dependence on the scattering direction. Then the conductivity becomes

$$\sigma_{xx} = \tau \frac{2e^2}{V} \frac{1}{N_k} \sum_k \left( -\frac{\partial f_k}{\partial \varepsilon_k} \right) (v_k)_x (v_k)_x = \tau \frac{2e^2 N(0)}{V} \langle v_x^2 \rangle \quad (84)$$

$\langle v_x^2 \rangle$  denotes the Fermi-surface average of  $(v_k)_x^2$ , and an isotropic average has been taken. Along these lines, first DFPT calculations for simple metals appeared already in 1998 [39].

## 4.5 Phonon-mediated pairing

Superconductivity is a macroscopic quantum phenomenon of the electron system. Its origin lies in an instability of the Fermi liquid state and leads to a new ground state of correlated paired electrons (Cooper pairs). The superconducting state has the important property that the quasiparticle spectrum is gapped. The size of the gap plays the role of an order parameter. In their seminal paper, Bardeen, Cooper, and Schrieffer (BCS) [40] have shown that this state is stabilized, whenever there exists an attractive interaction among two electrons. Such an attractive interaction is always provided by the electron-phonon coupling, which thus represents a natural source for pairing in any metal. EPC is known to be the pairing mechanism in most superconductors, which are commonly termed classical superconductors to distinguish them from more exotic materials where other types of pairing mechanism are suspected.

The BCS theory treated the EPC only in a simplified form appropriate for the weak coupling limit. A more complete theory has been soon after worked out applying many-body techniques (for a review see, e.g., Scalapino [41]). The resulting Eliashberg theory [42] extends the framework of BCS into the strong coupling regime and allows quantitative predictions.

Central to the theoretical formulation is a set of coupled equations, the so-called Eliashberg equations. A detailed derivation and justification of the approximations involved is given in the

review of Allen and Mitrovic [43]. One of its simplest form are the so-called *isotropic gap equations*. They are obtained by taking Fermi-surface averages of relevant quantities, i.e., ignoring the explicit momentum dependence, but keeping their frequency dependence. The justification comes from the observation that superconducting properties like the gap function are often very isotropic. In real materials, defects are always present and tend to average anisotropic gaps.

On the imaginary axis the isotropic gap equations read

$$\begin{aligned} i\omega_n(1-Z(i\omega_n)) &= -\pi T \sum_{n'} \Lambda(\omega_n-\omega_{n'}) \frac{\omega_{n'}}{\sqrt{\omega_{n'}^2+\Delta(i\omega_{n'})^2}} \\ \Delta(i\omega_n) Z(i\omega_n) &= \pi T \sum_{n'} \Lambda(\omega_n-\omega_{n'}) \frac{\Delta(i\omega_{n'})}{\sqrt{\omega_{n'}^2+\Delta(i\omega_{n'})^2}}. \end{aligned} \quad (85)$$

Here,  $\Delta(i\omega_n)$  is the frequency-dependent gap function and  $Z(i\omega_n)$  the frequency-dependent quasiparticle renormalization factor. The pairing interaction is encoded in the kernel

$$\Lambda(\nu_m) = \int d\omega \frac{2\omega\alpha^2 F(\omega)}{(\nu_m)^2 + \omega^2}, \quad (86)$$

where the electron-phonon coupling properties are described by the isotropic Eliashberg function

$$\alpha^2 F(\omega) = \frac{1}{N_q} \sum_q \delta(\omega-\omega_q) \frac{1}{N(0)} \frac{1}{N_k} \sum_{kk'} |g_{k'k}^q|^2 \delta(\varepsilon_k) \delta(\varepsilon_{k'}), \quad (87)$$

The isotropic Eliashberg function has the structure of a phonon density of states, weighted with squared EPC matrix elements averaged over states at the Fermi surface.

The set of non-linear equations (85) must be solved self-consistently for a given temperature  $T$  and pairing function  $\alpha^2 F$ . The superconducting state is characterized by a solution with  $\Delta(i\omega_n) \neq 0$ . The largest  $T$  which still allows such a solution defines the critical temperature  $T_c$ . The interaction kernel  $\Lambda(\nu_m)$  entering both equations is an even function of  $\nu_m$ . It takes its largest value at  $\nu_m = 0$

$$\lambda = \Lambda(0) = 2 \int d\omega \frac{\alpha^2 F(\omega)}{\omega}. \quad (88)$$

$\lambda$  is called the (isotropic) coupling constant and is a dimensionless measure of the average strength of the electron-phonon coupling. Depending on its value, materials are characterized as strong ( $\lambda > 1$ ) or weak coupling ( $\lambda < 1$ ). Due to the factor  $1/\omega$  in the integral, low-energy modes contribute more to the coupling strength than high-energy modes.

An important feature of the Eliashberg gap equations is that they only depend on normal-state properties, which specify a particular material. These comprise the electronic band structure, phonons, and the EPC vertex. Therefore, DFPT enables materials-specific predictions of superconducting properties from *first principles*.

One can establish a connection between  $\alpha^2 F$  and the phonon linewidths derived in the limit  $T \rightarrow 0$ , Eq. (70), namely

$$\alpha^2 F(\omega) = \frac{1}{2\pi N(0)} \frac{1}{N_q} \sum_q \frac{\gamma_q}{\omega_q} \delta(\omega-\omega_q), \quad (89)$$

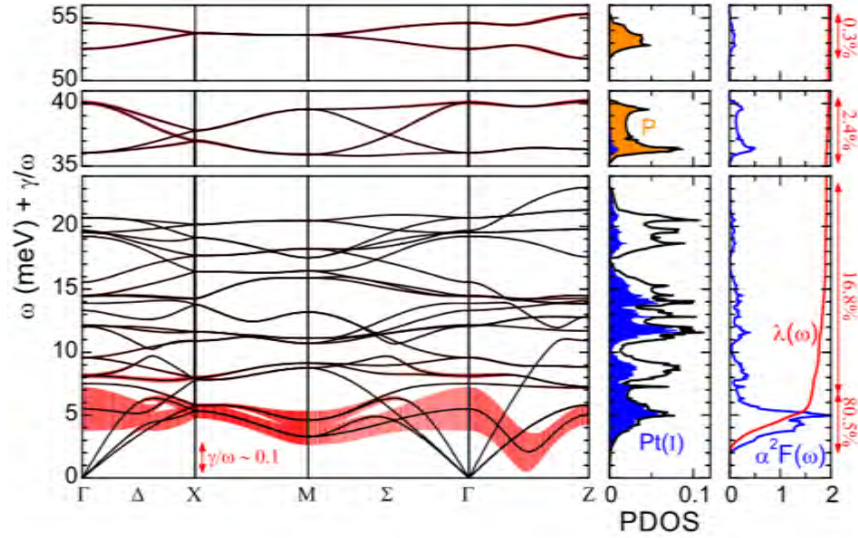


**Fig. 4:** DFPT results for the superconductor  $\text{SrPt}_3\text{P}$ . Left: phonon dispersion and relative linewidths (vertical red bars); middle: phonon density of states; right: calculated isotropic  $\alpha^2 F$ . DFPT predicts a soft, but strong-coupling phonon branch, which is the origin of the large peak in  $\alpha^2 F$  at low energies, and of a large coupling constant of  $\lambda \approx 2$ . After [46].

which leads to the formula for the isotropic coupling constant

$$\lambda = \frac{1}{\pi N(0)} \frac{1}{N_q} \sum_q \frac{\gamma_q}{\omega_q^2}. \quad (90)$$

The dimensionless prefactor  $\gamma_q/\omega_q$  in (89) can be interpreted as a measure of the coupling due to an individual phonon mode. The Eliashberg function is then given as a sum over all phonon branches and averaged over phonon momenta.

The residual Coulomb interaction among the quasiparticles can, however, not be completely neglected in the discussion of phonon-mediated superconductivity. It has a repulsive character and tends to reduce or completely suppress the pairing. It was shown by Morel and Anderson [44], that the Coulomb repulsion can be taken into account by replacing in the equation for the gap function the kernel by

$$A(i\omega_n - i\omega_{n'}) \rightarrow (A(i\omega_n - i\omega_{n'}) - \mu^*(\omega_c)) \Theta(\omega_c - |\omega_{n'}|). \quad (91)$$

A cutoff  $\omega_c$  is introduced which must be chosen to be much larger than phononic energies.  $\mu^*$  is called the effective Coulomb pseudopotential. In praxis,  $\mu^*$  is commonly treated as a phenomenological parameter of the order of  $\approx 0.1$  for normal metals. A more satisfactory approach, which actually allows to incorporate the Coulomb effects from *first principles*, is the density-functional theory of superconductors [45].

As an example, Fig. 4 shows results for the non-centrosymmetric, strong-coupling superconductor  $\text{SrPt}_3\text{P}$  ( $T_C = 8.4$  K). DFPT predicts that the pairing is driven mainly by a low-frequency mode, which carries more than 80% of the coupling. The existence of the low-frequency mode was confirmed by high-resolution inelastic X-ray experiments [46].

## 5 Extensions: LDA+U and beyond

In the previous Sections, we have demonstrated how the linear response technique is applied to the calculation of lattice dynamical properties and the evaluation of the electron-phonon vertex. This technique has been implemented for various band structure techniques. They usually rely on local approximations to the exchange-correlation functional (either LDA or GGA variants), which allows a straightforward evaluation of derivatives of the exchange-correlation potential  $v_{xc}$ . Yet, weaknesses of the local approximations are well known. Examples are an underestimation of band gaps in semiconductors, the failure to catch the long-range part of the van der Waals interaction, or the inadequate description of the Mott-Hubbard physics in strongly correlated materials. Various modifications have been proposed to improve these deficiencies. In many cases, they amount to a replacement of the local exchange-correlation potentials or functional by a more complex quantity, and thus has direct consequences for the evaluation of the linear response. In the following, we will use the DFT+U method, which is one of the simplest extension, as an example to discuss the type of complications arising in such schemes. At the end we will briefly touch more elaborate approaches.

The DFT+U method intends to improve the DFT description of electronic structures in the presence of pronounced local correlation. Examples are atoms with open  $d$  or  $f$  shells. The method has been introduced almost 30 years ago [47, 48] and is nowadays implemented in a variety of DFT codes. A more recent review can be found in [49].

Starting point is the definition of a correlated subspace, usually constructed from atom-like orbitals,  $\Phi_a(\mathbf{r})$ . The index  $a = (lm\sigma)$  represents a collection of quantum numbers characterizing the orbital. The DFT+U functional is expressed as

$$E = E_{\text{local}} + E_U. \quad (92)$$

$E_{\text{local}}$  is the DFT energy functional in a local approximation, i.e., with  $E_{XC}$  approximated by the LDA or GGA exchange-correlation energy.  $E_U$  is a correction of the form

$$E_U = \frac{1}{2} \sum_{abcd} \langle ab|v_c|cd \rangle (\rho_{ac}\rho_{bd} - \rho_{ad}\rho_{bc}) - E_{\text{dc}}[\{\rho_{ab}\}]. \quad (93)$$

$E_U$  is a function of the orbital density matrix of the correlated orbitals, which is calculated from the Kohn-Sham eigenstates  $\psi_i$  as

$$\rho_{ab} = \sum_i^{\text{occ}} \langle i|b \rangle \langle a|i \rangle. \quad (94)$$

$\langle ab|v_c|cd \rangle$  denotes the matrix elements of the Coulomb potential and thus encodes the local electron-electron interaction. There exists different variants of the functional form of this Coulomb kernel, but in all cases, it is expressed in terms of a few parameters only. The most common ones are  $U$  and  $J$ , which represent the effective Coulomb and exchange interactions, respectively.

The term  $E_{dc}$  is the famous *double counting* term which attempts to correct for the fact that  $E_{\text{local}}$  already contains part of the local electron-electron interaction. Different expressions for the *double counting* term exist, but it is always given by a quadratic polynomial in  $\rho_{ab}$ .

The Kohn-Sham equations are augmented by an additional potential

$$v_{\text{eff}} = v_{\text{ext}} + v_{\text{scr}}[n(\mathbf{r})] + \hat{v}_U[\{\rho_{ab}\}] \quad (95)$$

given by

$$\hat{v}_U = \sum_{ab} v_{ab} |a\rangle\langle b| = \sum_{ab} v_{ab} \hat{Q}_{ab} \quad (96)$$

with

$$v_{ab} = \frac{\delta E_U}{\delta \rho_{ba}} = \sum_{cd} (\langle ac|v_c|bd\rangle - \langle ad|v_c|cb\rangle) \rho_{cd} - (v_{dc})_{ab}. \quad (97)$$

$\hat{v}_U$  is a non-local operator containing the operator  $\hat{Q}_{ab} = |a\rangle\langle b|$  of the local correlated subspace. When solving the self-consistent Kohn-Sham equations,  $\rho_{ab}$  can formally be considered as additional degrees of freedom besides the density  $n(\mathbf{r})$ . In each step, after solving the Kohn-Sham equation to obtain the KS wave functions, both the density and the orbital density matrix are updated, and finally a new effective potential is calculated with the help of Eqs. (96) and (97). What are the consequences for the linear-response calculations? Let us first consider the linear change of the orbital density matrix under an external adiabatic perturbation. It consists of two parts

$$\delta \rho_{ab} = \delta \rho_{ab}^{(el)} + \delta \rho_{ab}^{(b)} \quad (98)$$

with

$$\begin{aligned} \delta \rho_{ab}^{(el)} &= \sum_i^{\text{occ}} \left( \{ \delta \langle i| \} \hat{Q}_{ba} |i\rangle + \langle i| \hat{Q}_{ba} \{ \delta |i\rangle \} \right) \\ \delta \rho_{ab}^{(b)} &= \sum_i^{\text{occ}} \langle i| \delta \hat{Q}_{ba} |i\rangle. \end{aligned} \quad (99)$$

$\delta \rho_{ab}^{(el)}$  results from the variation of the KS wave functions, while  $\delta \rho_{ab}^{(b)}$  derives from a change of the local basis by the perturbation. The latter comes into play when a perturbation modifies the correlated subspace. This happens, for example, when an atom is displaced and the correlated subspace attached to this atom is moved along.

Derivatives of the total energy involve additional contributions from  $E_U$ . In first order it reads as

$$\frac{\partial E}{\partial \lambda} \rightarrow \sum_{ab} \frac{\delta E_U}{\delta \rho_{ab}} \left( \frac{\partial \rho_{ab}^{(b)}}{\partial \lambda} \right). \quad (100)$$

This form is a consequence of the Hellmann-Feynman theorem, which ensures, that no contribution from the first-order variation of the wave functions enters. Only the explicit dependence of the correlated subspace on the perturbation plays a role. This is not true anymore for the second derivative of the energy

$$\frac{\partial^2 E}{\partial \lambda_1 \partial \lambda_2} \rightarrow \sum_{abcd} \frac{\delta^2 E_U}{\delta \rho_{ab} \delta \rho_{cd}} \left( \frac{\partial \rho_{ab}^{(b)}}{\partial \lambda_1} \right) \left( \frac{\partial \rho_{cd}}{\partial \lambda_2} \right) + \sum_{ab} \frac{\delta E_U}{\delta \rho_{ab}} \frac{\partial}{\partial \lambda_2} \left( \frac{\partial \rho_{ab}^{(b)}}{\partial \lambda_1} \right). \quad (101)$$

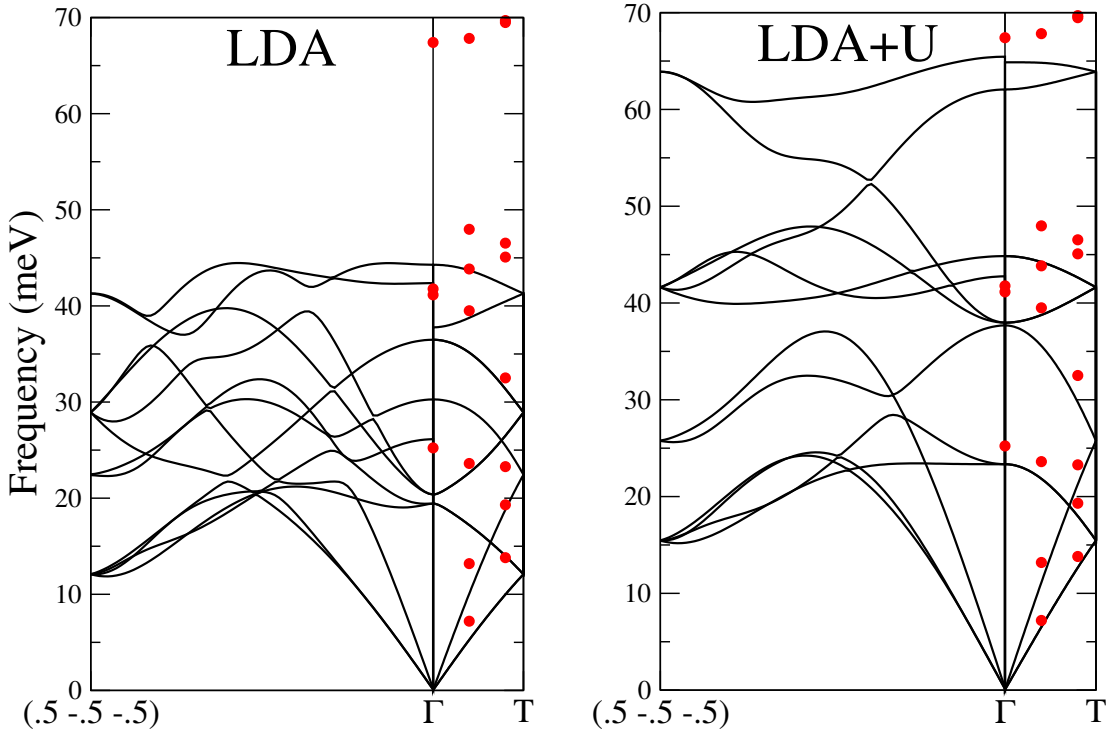


**Fig. 5:** Phonon dispersion of NiO for LDA (left panel) and LDA+U (right panel) using  $U=5$  eV. Experimental data (red circles) are taken from [51].

Both terms now contain first-order variations of the KS wave functions. They are solutions of the linear Eq. (27), but with  $\delta v_{\text{eff}}$  augmented by an additive contribution from the orbital density matrix

$$\delta v_{\text{eff}}(\mathbf{r}) = \delta v_{\text{ext}}(\mathbf{r}) + \int d^3 r' I(\mathbf{r}, \mathbf{r}') \delta n(\mathbf{r}') + \sum_{abcd} I_{ab,cd} \delta \rho_{cd} \hat{Q}_{ab} + \sum_{ab} v_{ab} \delta \hat{Q}_{ab}, \quad (102)$$

where

$$I_{ab,cd} = \frac{\partial v_{ab}}{\partial \rho_{cd}} = \frac{\partial^2 E_U}{\partial \rho_{ab} \partial \rho_{cd}}. \quad (103)$$

Combined with Eq. (99) this closes the DFPT self-consistency cycle. The above expressions exhibit an increased complexity as compared to the standard DFPT. This is the reason why up to now, only one implementation has been reported [50].

Finally, the EPC vertex can be corrected by taking into account both the modified wave functions and the augmented change of the effective potential (102).

The effect of the +U correction can be quite dramatic not only for electronic structure, but also for derived quantities like the lattice dynamics. An example is given in Fig. 5, which compares the phonon spectrum of NiO obtained with LDA and LDA+U. NiO is a textbook example of a charge-transfer insulator, where local correlations in the open  $d$  shell of Ni are decisive. In its ground state, it orders antiferromagnetically along the cubic [111] direction of the rock-salt structure, and possesses a large optical gap of 3.1 eV. While LDA can reproduce the AF state, it severely underestimates the gap (0.4 eV). The gap is increased by adding the +U correction.

For a test calculation with  $U = 5$  eV, the gap increases to 2.8 eV. At the same time, the phonon spectrum hardens significantly (see Fig. 5). Its origin lies in an effectively reduced screening when the LDA+U correction is applied. This significantly improves agreement with experiment. Similar trends were also found for MnO [50].

To conclude this Section, we will take a brief look at more advanced corrections to the local approximation in DFT, and discuss recent attempts to use them in linear response and electron-phonon interaction. Three classes will be considered:

1. Hybrid functionals: the local approximation to the exchange energy,  $E_X(n)$ , is replaced by the exact, non-local exchange. This corrects some deficiencies of the local approximations, and improves the description of wave functions and energies (e.g. gaps in semiconductors). The prize to pay is a drastically increased numerical effort in evaluating both exchange energy and potential, preventing up to now a full DFPT implementation. Phonons and EPC have been addressed using frozen phonon techniques [52–54], but they require the use of supercells and give only limited information on the momentum dependence.
2. GW approach: the KS equations describe a fictitious system of non-interacting electrons, and KS states differ in general from the true quasiparticle wave functions and energies. The latter are determined from a quasiparticle equation, which replaces  $v_{XC}$  in the KS equation by a self-energy operator  $\hat{\Sigma}$ . The GW method evaluates  $\hat{\Sigma}$  based on the lowest-order term of the electron-electron interaction.  $\hat{\Sigma}$  is expressed in terms of the Green function “G”) and screened electron-electron interaction (“W”). This approach, too, is numerically very expensive, but improves the description of quasiparticle properties. It has been used to improve the EPC vertex in the context of frozen-phonon techniques [53]. Very recently a more elaborate linear-response formulation was developed [55]. It starts from a LDA/GGA self-consistent DFPT calculation to obtain the first-order change of the KS wave functions. This is subsequently used to calculate  $\delta\hat{\Sigma}$  and to correct the EPC vertex via

$$\delta v_{\text{eff}}^{GW} = \delta v_{\text{eff}}^{DFT} - \delta v_{XC} + \delta\hat{\Sigma}. \quad (104)$$

This perturbative scheme has the advantage to get the EPC matrix elements for arbitrary momenta without the need of a supercell.

3. DFT + Dynamical mean-field theory (DMFT): local correlations are cast into a frequency-dependent self-energy  $\Sigma(\omega)$  by solving a many-body impurity problem. The impurity system is embedded in a crystalline environment, whose electronic structure is described by DFT. Kotliar and coworkers developed a formulation based on a generating functional, from which both DFT and DMFT equations are derived in a unified framework [56]. Based on this description, a linear response approach has been formulated and applied to a lattice dynamical properties [57]. The method is, however, involved and numerically challenging.

## 6 Summary

The purpose of this tutorial was to give an introduction into modern linear-response techniques, give access to fundamental properties of electrons, phonons, and their interactions from first principles. In many respects, this approach has matured into a powerful tool, which is applied routinely to a large variety of material classes. We have also discussed examples of physical quantities, which are influenced or even determined by EPC in a direct way, thus providing experimental probes to critically assess theoretical predictions. While for many compounds DFPT predictions for the EPC strength turn out to be rather reliable, larger deviations are expected in cases, when standard DFT already fails to properly describe the electronic subsystem. First promising steps have been taken to incorporate more sophisticated treatments of electron correlations in order to improve the description of EPC in systems, where strong correlations play a crucial role.

## References

- [1] P. Hohenberg and W. Kohn, *Phys. Rev.* **B136**, 864 (1964)
- [2] W. Kohn and L.J. Sham, *Phys. Rev.* **A140**, 1133 (1965)
- [3] R.M. Dreizler and E.K.U. Gross: *Density Functional Theory: An Approach to the Quantum Many-Body Problem* (Springer, Berlin, 1990)
- [4] R.O. Jones and O. Gunnarsson, *Rev. Mod. Phys.* **61**, 689 (1989)
- [5] R.G. Parr and W. Yang: *Density-Functional Theory of Atoms and Molecules* (Oxford University Press, New York, 1989)
- [6] D.C. Langreth and M.J. Mehl, *Phys. Rev. B* **28**, 1809 (1983)
- [7] J.P. Perdew, K. Burke, and M. Ernzerhof, *Phys. Rev. Lett.* **77**, 3865 (1996)
- [8] J.P. Perdew, K. Burke, and M. Ernzerhof, *Phys. Rev. Lett.* **78**, 1396 (1997)
- [9] R.P. Feynman, *Phys. Rev.* **56**, 340 (1939)
- [10] X. Gonze and J.-P. Vigneron, *Phys. Rev. B* **39**, 13120 (1989)
- [11] X. Gonze, *Phys. Rev. A* **52**, 1086 (1995)
- [12] X. Gonze, *Phys. Rev. A* **52**, 1096 (1995)
- [13] M.S. Hybertsen and S.G. Louie, *Phys. Rev. B* **35**, 5585 (1987)
- [14] N.E. Zein, *Sov. Phys. Solid State* **26**, 1825 (1984)
- [15] D.K. Blat, N.E. Zein, and V.I. Zinenko, *J. Phys. Condens. Matt.* **3**, 5515 (1991)
- [16] N.E. Zein, *Phys. Lett. A* **161**, 526 (1992)
- [17] S. Baroni, P. Giannozzi, and A. Testa, *Phys. Rev. Lett.* **58**, 1861 (1987)
- [18] P. Giannozzi, S. de Gironcoli, P. Pavone, and S. Baroni, *Phys. Rev. B* **43**, 7231 (1991)
- [19] S. Baroni, S. de Gironcoli, A. Dal Corso, and P. Giannozzi, *Rev. Mod. Phys.* **73**, 515 (2001)
- [20] M. Born and J.R. Oppenheimer, *Ann. Physik* **84**, 457 (1927)
- [21] G.V. Chester and A. Houghton, *Proc. Phys. Soc.* **73**, 609 (1959)
- [22] M. Born and K. Huang: *Dynamical Theory of Crystal Lattices* (Clarendon Press, Oxford, 1954)

- [23] A.A. Maradudin, E.W. Montroll, G.H. Weiss, and I.P. Ipatova: *Solid State Physics, Supplement 3* (Academic Press, New York, 1971), p. 1
- [24] H. Boettger: *Principles of the Theory of Lattice Dynamics* (Physik Verlag, Weinheim, 1983)
- [25] G. Grimvall: *The Electron–Phonon Interaction in Metals* in E. Wohlfarth (ed.): *Selected Topics in Solid State Physics* (North-Holland, New York, 1981)
- [26] G.D. Mahan: *Many-Particle Physics*, (Plenum Press, New York, 1990)
- [27] R. Heid, I.Yu. Sklyadneva, and E.V. Chulkov, *Sci. Rep.* **7**, 1095 (2017)
- [28] P.B. Allen, *Phys. Rev. B* **6**, 2577 (1972)
- [29] F. Weber, S. Rosenkranz, L. Pintschovius, J.-P. Castellan, R. Osborn, W. Reichardt, R. Heid, K.-P. Bohnen, E.A. Goremychkin, A. Kreyssig, K. Hradil, and D. Abernathy, *Phys. Rev. Lett.* **109**, 057001 (2012)
- [30] F. Weber, L. Pintschovius, W. Reichardt, R. Heid, K.-P. Bohnen, A. Kreyssig, D. Reznik, and K. Hradi, *Phys. Rev. B* **89**, 104503 (2014)
- [31] J.M. Ziman: *Electrons and phonons: the theory of transport phenomena in solids* (Clarendon, Oxford, 1960)
- [32] F. Giustino, *Rev. Mod. Phys.* **89**, 015003 (2017)
- [33] T. Sohler, M. Calandra, C.-H. Park, N. Bonini, N. Marzari, and F. Mauri, *Phys. Rev. B* **90**, 125414 (2014)
- [34] W. Li, *Phys. Rev. B* **92**, 075405 (2015)
- [35] M. Fiorentini and N. Bonini, *Phys. Rev. B* **94**, 085204 (2016)
- [36] P.B. Allen, *Phys. Rev. B* **3**, 305 (1971)
- [37] P.B. Allen, *Phys. Rev. B* **13**, 1416 (1976)
- [38] P.B. Allen, W.E. Pickett, and H. Krakauer, *Phys. Rev. B* **37**, 7482 (1988)
- [39] R. Bauer, A. Schmid, P. Pavone, and D. Strauch, *Phys. Rev. B* **57**, 11276 (1998)
- [40] J. Bardeen, L.N. Cooper, and J.R. Schrieffer, *Phys. Rev.* **108**, 1175 (1957)
- [41] D.J. Scalapino: *The Electron-Phonon Interaction and Strong-Coupling* in R.D. Parks (ed.): *Superconductivity, Vol. 1* (Dekker, New York, 1969)
- [42] G.M. Eliashberg, *Zh. Eksp. Fiz.* **38**, 966 (1960) [*Sov. Phys. JETP* **11**, 696 (1960)]

- 
- [43] P.B. Allen and B. Mitrović, *Solid State Physics* **37**, 1 (1982)
- [44] P. Morel and P.W. Anderson, *Phys. Rev.* **125**, 1263 (1962)
- [45] L.N. Oliveira, E.K.U. Gross, and W. Kohn, *Phys. Rev. Lett.* **50**, 2430 (1988)
- [46] D.A. Zocco, S. Krannich, R. Heid, K.-P. Bohnen, T. Wolf, T. Forrest, A. Bosak, and F. Weber, *Phys. Rev. B* **92**, 220504 (2015)
- [47] V.I. Anisimov and O. Gunnarsson, *Phys. Rev. B* **43**, 7570 (1991)
- [48] V.I. Anisimov, J. Zaanen, and O.K. Andersen, *Phys. Rev. B* **44**, 943 (1991)
- [49] B. Himmetoglu, A. Floris, S. de Gironcoli, and M. Cococcioni, *Int. J. Quantum Chem.* **114**, 14 (2014)
- [50] A. Floris, S. de Gironcoli, E.K.U. Gross, and M. Cococcioni, *Phys. Rev. B* **84**, 161102(R) (2011)
- [51] W. Reichardt, V. Wagner, and W. Kress, *J. Phys.* **C8**, 3955 (1975)
- [52] C.H. Patterson, *Phys. Rev. B* **77**, 115111 (2008)
- [53] Z.P. Yin, A. Kutepov, and G. Kotliar, *Phys. Rev. X* **3**, 021011 (2013)
- [54] B. Pamuk, J. Baima, R. Dovesi, M. Calandra, and F. Mauri, *Phys. Rev. B* **94**, 035101 (2016)
- [55] Z. Li, G. Antonius, M. Wu, F.H. da Jornada, and S.G. Louie, *Phys. Rev. Lett.* **122**, 186402 (2019)
- [56] G. Kotliar, S.Y. Savrasov, K. Haule, V.S. Oudovenko, O. Parcollet, and C.A. Marianetti, *Rev. Mod. Phys.* **78**, 865 (2006)
- [57] S.Y. Savrasov and G. Kotliar, *Phys. Rev. Lett.* **90**, 056401 (2003)

